Carbohydrate Polymers 97 (2013) 217–225

Contents lists available at SciVerse ScienceDirect

Carbohydrate Polymers

journal homepage: www.elsevier.com/locate/carbpol

Carvacrol affects interfacial, structural and transfer properties of chitosan coatings applied onto polyethylene

Mia Kurek[a,b], Claire-Hélène Brachais[d], Mario Ščetar[b], Andrée Voilley[a], Kata Galić[b], Jean-Pierre Couvercelle[d], Frédéric Debeaufort[a,c,*]

[a] PAM-PAPC, 1 Esplanade Erasme, Université de Bourgogne – Agrosup Dijon, F-21000 Dijon, France
[b] Laboratory for Food Packaging, Faculty of Food Technology and Biotechnology, University of Zagreb, HR-10000 Zagreb, Croatia
[c] IUT-Dijon Departement Genie Biologique, 7 Boulevard Dr. Petitjean, B.P. 17867, F-21078 Dijon Cedex, France
[d] ICMUB UMR-CNRS 5260, EMMD, 9 Allée Alain Savary, F-21000 Dijon, France

ARTICLE INFO

Article history:
Received 8 March 2012
Received in revised form 16 April 2013
Accepted 17 April 2013
Available online 30 April 2013

Keywords:
Bio-based polymer
Coating
Chitosan
Wettability
Surface energy
Permeability

ABSTRACT

Different chitosan coating solutions were tested with the aim of investigating their adhesion and wettability onto polyethylene film to improve packaging performance and provide antimicrobial properties. Surface wetting kinetics was monitored by contact angle measurements. Addition of ethanol and carvacrol improved wettability and adhesion of the thin chitosan layer. Structure, water vapour, O_2, CO_2 and air permeabilities of self supported chitosan films and coated polyethylene were determined. The formation of a thin chitosan layer on polyethylene improved gas barrier properties decreasing the Permeability Coefficient for oxygen and carbon dioxide (P_{O_2}, P_{CO_2}) from 100 to 10,000 times. Presence of carvacrol in the chitosan coating layer increased P_{O_2}, P_{CO_2} and P_{air} by a factor of ten. Moreover, it influenced film microstructure. However chitosan was shown to be good gas barrier film in the dry state.

1. Introduction

The combination of bio-based polymers with common synthetic materials is a novel approach in material engineering that has significantly increased over the past few years (Farris et al., 2011). Derived from various natural sources bio-based polymers can be formed as either coatings or self standing films (Hong & Krochta, 2006). Still, the replacement of plastics with a self standing bio-based polymer is a difficult task to achieve. Therefore development of new bio-based coatings or internal layers to improve barrier, thermal and mechanical properties has been proposed (Farris et al., 2011; Hong, Lee, & Krochta, 2005).

The wettability of a solid surface is one of the crucial parameters in the production of composite coated materials. Moreover it is of a great importance for industrial application. Surface layer properties, wettability, surface free energy and phenomena that occur at the interfaces are important criteria for the efficiency of the adhesion properties of the coatings onto polymers (Zenkiewicz, 2007). The similarity between the coating solution and the surface to be coated in values of dispersive and polar components influences the spreadability of the coating solutions. A better compatibility between the coated surface and the coating film forming solutions can be achieved by incorporating surface-active agents within the casting solution. Chitosan is a functional bio-based polymer with a great potential in food applications. It is due to its biodegradability, biocompatibility, antimicrobial activity, nontoxicity and film forming capacity (Arvanitoyannis, 1999; Tharanathan & Kittur, 2003). Chitosan based films are good oxygen and carbon dioxide barriers. Still, due to its hydrophilic nature, they are highly permeable to water vapour (Suyatma, Copinet, Tighzert, & Coma, 2004).

Due to the health concerns and environmental problems, the current research on active packaging has focused on natural preservatives or natural active compounds introduced into biodegradable/biosourced packaging materials (Siripatrawan & Harte, 2010; Suppakul, Miltz, Sonneveld, & Bigger, 2003). Therefore, the incorporation of carvacrol as the main component from oregano essential oil can improve both the antimicrobial and the functional film properties (Vargas, Albors, Chiralt, & González-Martínez, 2009).

When designing the most suitable film for a determined use, it is important to understand the influence of physico-chemical factors on the functional properties of the film forming solutions

* Corresponding author at: UMR PAM-PAPC, 1 Esplanade Erasme, Université de Bourgogne – AgroSup Dijon, F-21000 Dijon, France. Tel.: +33 380 39 6547; fax: +33 380 77 4047.
E-mail address: frederic.debeaufort@u-bourgogne.fr (F. Debeaufort).

0144-8617/$ – see front matter © 2013 Elsevier Ltd. All rights reserved.
http://dx.doi.org/10.1016/j.carbpol.2013.04.059

and obtained films. The application target of this research was the development of the environmentally friendly carvacrol activated chitosan-coated polyethylene film. Carvacrol was incorporated in the coating layer with the purpose of creating an active antimicrobial film for further application. Furthermore, it is aimed to assess the ability of the deposition of different compositions of chitosan coatings on the low density polyethylene. Therefore, surface modifications and barrier property changes after the coating process have been studied as a function of the coating composition. To better understand the possible changes in the chitosan coatings and in the chitosan self standing films have also been studied.

2. Materials and methods

2.1. Materials and reagents

Commercial grade chitosan (CS) (France Chitine, Marseille, France, powder 652, having a molecular mass of 165 kDa, degree of deacetylation of >85%) was used as the film forming matrix. A commercial, low density polyethylene film (LDPE) (Wipak, Lille, LDPE45 UFP; thickness of 45 μm) was used as a polyolefin material. Carvacrol (CVC) (purity >97%, Fluka) was used as the aroma compound in order to improve the functional film properties. Acetic acid (glacial 100%, Merck, Darmstadt, Germany) and pure ethanol (absolute, Sigma–Aldrich) were used as solvents in the preparation of the film forming solutions (FFS). Magnesium chloride ($MgCl_2$, Sigma) was used to prepare saturated salt solutions to fix the relative humidity for water vapour permeability measurements. Deionised water, diodomethane (purity >99%, Sigma–Aldrich), glycerol (Fluka Chemical, 98% purity, Germany) and tetradecane (purity >99%, Sigma–Aldrich) were used for surface analysis. No further purification of chemicals has been done and freshly prepared solutions were always used.

2.2. Film preparation

2.2.1. Self standing chitosan films

A chitosan solution was prepared by dissolving the chitosan powder in a 1% (v/v) aqueous acetic acid, to obtain 2% (w/v) film forming solutions (FFS). To achieve a complete dispersion of chitosan, the solution was stirred for 2 h at room temperature. To prepare aqueous hydroalcoholic acid media, ethanol was mixed in a ratio ethanol:aqueous acetic acid of 30:70. To obtain film forming solutions with incorporated aroma compound, carvacrol (0.5%, w/v) was homogenised either in aqueous acid CS solution or hydroalcoholic acid CS solution at 24,000 rpm for 10 min with an Ultra Turrax (T25 IKA). In order to obtain films, solvents were removed by drying in a ventilated climatic chamber (KBF 240 Binder, ODIL, France) at 20 °C and 30% RH. After drying, the films were peeled off and stored in the same ventilated climatic chamber at 25 °C and 30% RH before measurements. The films prepared in the acetic acid solution were coded as CSA, those in hydroalcoholic acid solution as CSE and those containing carvacrol as CVC.

2.2.2. Chitosan coated polyethylene films

The hydroalcoholic acid chitosan solution with/or without carvacrol was prepared as described in Section 2.2.1. Chitosan coated PE were prepared according to Sollogoub et al. (2009). The coating was carried out at room temperature, using a Nordson slot die (ChameleonTM), appropriate to fluids of viscosity ranging between 0.5 and 2 Pa/s. Films were dried in a flow of a dry air at 50 °C and RH < 10%. After drying, they were stored in a ventilated climatic chamber (KBF 240 Binder, ODIL, France) before measurements at 25 °C and 30% RH.

2.3. Contact angle, surface tension, critical surface tension, surface free energy and wettability measurements

2.3.1. Determination of a contact angle

Contact angle (θ) is described as a relationship between the surface tension at a point of the three phase contact line between a solid phase S, a liquid L and its vapour V given by:

$$\gamma_{LV} \times \cos\theta = \gamma_{SV} - \gamma_{SL} \quad (1)$$

where γ_{LV}, γ_{SV} and γ_{SL} are the surface tensions of the liquid–vapour, solid–vapour and solid–liquid, respectively (Young, 1805).

The contact angle was measured by the sessile drop method, in which a droplet of the tested liquid was placed on a horizontal film surface. Measurement was done using a DGD-DX goniometer (GBX, Romans-sur-Isere, France), equipped with the DIGIDROP image analysis software (GBX, Romans-sur-Isere, France) according to Karbowiak, Debeaufort, and Voilley (2006). A droplet of a testing solution (~1.5 μL) was deposited on the film surface with a precision syringe. The contact angles were measured on both sides of the drop and averaged. The measurement was carried on over 120 s. The effect of evapouration was assessed on the aluminium foil considered as an impermeable reference surface. All measurements were done on both sides of the films. For chitosan self supported films, the surface in contact with the glass support during drying will be referred to as the "support side" and the other surface in contact with the air during drying will be referred to as the "air side".

2.3.2. Surface tension and critical surface tension determination

The surface tension of the film forming (coating) solutions (γ_L) was measured by the sessile drop method and Laplace–Young approximation (Song & Springer, 1996a,b). In order to determine the drop shape, using the image analysing software, solutions were taken with a 1 mL syringe (Hamilton, Switzerland). The estimation of the critical surface tension (γ_C) of the PE, the coated PE and the self standing chitosan films was obtained by extrapolation from the Zisman plot (Zisman, 1964). Zisman plots were obtained by plotting the cosine of the contact angles ($\cos\theta$) of a series of standard liquids (Table 1) on the film surface versus the surface tension of the same liquids. The critical surface tension values of films are the mean of the extrapolation of $\cos\theta$ for the liquids that form approximately a straight line. Extrapolation of this line to the point of $\cos\theta = 1$, yields the value of the critical surface energy equal to liquid surface tension (γ_L) at this point.

2.3.3. Surface free energy and wettability

The surface free energy (SFE) and its polar (γ_S^P) and dispersive (γ_S^D) components were calculated by the Owens–Wendt method (Owens & Wendt, 1969), according to Eqs. (2) and (3):

$$\gamma_S = \gamma_S^D + \gamma_S^P \quad (2)$$

$$\gamma_L(1 + \cos\theta) = 2\left((\gamma_S^D\gamma_L^D)^{0.5} + (\gamma_S^P\gamma_L^P)^{0.5}\right) \quad (3)$$

Because two unknowns, γ_S^D and γ_S^P appear in Eq. (3), it is insufficient to determine the SFE of a polymer. Thus, the contact angle has to be measured using two measuring liquids of known surface tension and their polar (γ_L^P) and dispersive (γ_L^D) component (deionised water as the liquid with the dominant polar component and diodomethane with the dominant dispersive component). That yields to the two equations in the form of Eq. (2), with different

Table 1
Surface tension (γ_L) and dispersive (γ_L^D) and polar (γ_L^P) surface tension components and adhesion (W_a), cohesion (W_c) and spreading coefficient (W_s) of standard liquids and chitosan film forming solutions (FFS) on the PE at equilibrium after 30 s (Θ_{30s}).

Compound	γ_L (mN/m)	γ_L^D (mN/m)	γ_L^P (mN/m)	W_A	W_C	W_S	Θ_{30s}
Water[a]	72.8	21.8	51.0	82.4b	145.6a	−63.2g	82.4 ± 4.8a
Diodomethane[a]	50.8	50.8	0	79.7b,c,d	101.6f	−21.9d	55.3 ± 1.5c
Glycerol[a]	64.0	34.0	30.0	86.4a	128.0d	−41.6f	69.5 ± 7.7b
Tetradecane[a]	26.6	26.6	0	49.9g	53.1j	−3.2a	28.6 ± 2.5e
Hydroalcoholic acid solution	55.0	ND	ND	76.4d	110.0e	−33.6e	67.1 ± 3.6b
Aqueous acetic acid solution	70.0	ND	ND	78.2c,d	140.0c	−61.8g	83.2 ± 1.3a
CSA-FFS	71.7	ND	ND	80.1b,c	143.5 b	−63.4a	83.3 ± 3.5a
CSE-FFS	32.4	ND	ND	57.4e,f	64.8h	−7.4b	39.4 ± 2.6d
CSACVC-FFS	37.9	ND	ND	59.8e	75.8g	−15.9c	54.6 ± 0.2c
CSECVC-FFS	31.3	ND	ND	55.6f	62.6i	−6.9b	39.0 ± 1.6d,e

ND not detected.
Different letters indicate a statistically significant difference.
CSA-FFS – chitosan in aqueous acid solution; CSE-FFS – chitosan in hydroalcoholic acid solution; CSACVC-FFS – chitosan and carvacrol in aqueous acid solution; CSECVC-FFS – chitosan and carvacrol in hydroalcoholic acid solution.
[a] Adapted from Van Oss (1994).

values of the constant coefficients. As a result, a system of two linear equations is obtained:

$$(\gamma_S^D)^{0.5} + a(\gamma_S^P)^{0.5} = b(1+\cos\,\theta_1)$$
$$(\gamma_S^D)^{0.5} + c(\gamma_S^P)^{0.5} = d(1+\cos\,\theta_2) \quad (4)$$

where a, b, c, d are the coefficients dependent on the types of these liquids and θ_1 and θ_2 are contact angles of water and diodomethane over a tested film.

When considering the attractive forces at a given interface, it has been suggested that the liquid–vapour interfacial tension is the sum of contributions from the different intermolecular forces (Kaelble, 1970; Rabel, 1971; Dupre, 1869). For a pure liquid, if polar and dispersive interactions are known, and if the contact angle between that liquid and a solid is obtained, the interaction can be described by the adhesion coefficient (work of adhesion per unit area, W_a), given by Dupre equation (Dupre, 1869):

$$W_a = W_a^D + W_a^P \leftrightarrow 2((\gamma_S^D\gamma_L^D)^{0.5} + (\gamma_S^P\gamma_L^P)^{0.5}) = \gamma_L(1+\cos\,\theta) \quad (5)$$

and the cohesion coefficient (work of cohesion per unit area, W_c), given by:

$$W_c = 2\gamma_{LV} \quad (6)$$

Then, spreading coefficient (W_s) for a liquid over a solid is calculated as:

$$W_s = W_a - W_c = \gamma_{SV} - \gamma_{LV} - \gamma_{LS} \quad (7)$$

The physical significance of this energy change is the work needed to separate the solid and liquid from the solid/liquid interface. The equilibrium spreading coefficient can only be negative or equal to zero.

2.4. Gas permeability measurements

The gas permeability determination was performed using a manometric method, on a permeability testing appliance, Brugger, Type GDP-C (Brugger Feinmechanik GmbH, Germany). The increase in pressure during the test period was assessed and displayed by an external computer. The data were recorded and the permeance was calculated by a GDP-C Software with temperature compensation. The sample temperatures were adjusted using an external Thermostat (HAAKE F3 with Waterbath K). The temperature dependence of the permeability was modelled using Arrhenius equations to determine the activation energy for permeation (E_a, J/mol):

$$P = P_0 \exp\left(\frac{-E_a}{RT}\right) \quad (8)$$

where P_0 is pre-exponential factor, R is gas constant (8.31 J/mol K), and T is temperature (K).

2.5. Water vapour permeability measurement (WVP)

The film thickness was measured with an electronic gauge (Posi-Tector 6000, DeFelsko Corporation, USA). The average value of five thickness measurements per type of film was used in all the WVP calculations (statistical error on the film thickness is added in WVP uncertainty). The WVP of films was determined gravimetrically using a modified ASTM E96-80 (1980) standard method, adapted to edible materials by Debeaufort, Martin-Polo, and Voilley (1993), using the relative humidity differential of 0–33% RH and the temperature of 25 ± 1 °C. Prior to the WVP measurements, all the film samples were equilibrated at 25 ± 1 °C and RH 30% for 72 h. The film samples were then placed between two Teflon rings on the top of the glass cell containing a salt solution of $MgCl_2$ (RH ~ 33%) and the cells were stored at RH ~ 0% over a silica gel. These permeation cells were introduced into a ventilated chamber (KBF 240 Binder, ODIL, France) maintained at 25 ± 1 °C. The 0–33% RH gradient was chosen to lower as much possible the plasticising effect of water on chitosan (Ziani, Oses, Coma, & Maté, 2008) and then to allow the display of plasticisation/antiplasticisation of film components. WVP (g/m s Pa) was calculated, from the change in the cell weight versus time at the steady state, using the following equation:

$$\mathrm{WVP} = \frac{\Delta m}{\Delta t \times \Delta p \times A} \times e \quad (9)$$

where $\Delta m/\Delta t$ is the weight of moisture loss per unit of time (g/s), A is the film area exposed to the moisture transfer (9.08×10^{-4} m^2), e is the film thickness (m), and Δp is the water vapour pressure difference between the two sides of the film (Pa). Three replicates for each film type were done.

2.6. Film microstructure

The film microstructure was examined using environmental scanning electron microscopy (ESEM, Philips XL 30 ESEM, Japan). A 5 mm × 10 mm film was fixed on the support using a double side adhesive tape with an angle of 90° to the surface to allow the observation of the film cross section. All the films were cut with a new razor blade to prevent as much as possible any morphological damage. The films were observed at different magnifications up to ×15,000 for focusing and images were taken at magnification from 800× to 8000× with an intensity of 8 kV and absolute pressure of 230 Pa (RH ~ 30% at 5 °C).

2.7. Statistical analysis

The statistical analysis of the data was performed through variance analysis (ANOVA) using Xlstat-Pro (win) 7.5.3. (Addinsoft, New York). The data were ranked and statistical differences were evaluated on the ranks with a one-way analysis of variance (ANOVA) and Tukey's multiple comparison tests. In all cases, a value of $p < 0.05$ was considered to be significant.

3. Results

3.1. Spreading of FFS and wettability of PE

This experiment was designed to study the compatibility of the chitosan film forming solutions (FFS) and the PE that was used as support film. First of all, to ensure adequate bonding, spreading and wetting, FFS should have a liquid surface tension higher than the critical surface tension (γ_C) of the support PE film. γ_C was extrapolated from Zisman plot (Fig. 1). The compatibility of the surface polarity and FFS played an important role in the PE wettability. The evaluation of γ_C and surface free energy through the surface forces measurement is an approach that quantifies the "surface affinity" for solutions. PE film was shown to be a low energy surface (35 mN/m) with a higher dispersive (31.3 mN/m) and a lower polar (4.4 mN/m) component (Table 2). This denotes the ability of PE to participate in non-polar interactions. Thus, a surface with these characteristics interacts with the liquid primarily by dispersion forces and influences the effective spreading of the coating on the PE surface (Rulon & Robert, 1993). Table 1 shows the surface tensions of four different film forming solutions, two solvents used to solubilise chitosan powder and four standard liquids applied on PE for design of the Zisman plots.

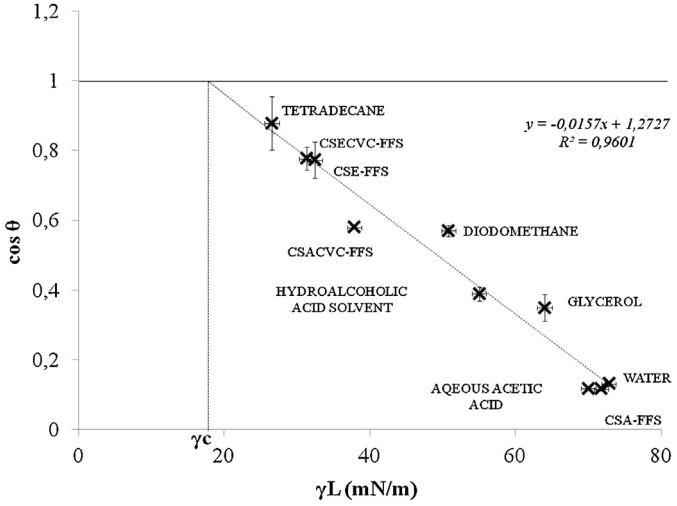

Fig. 1. Zisman plot of polyethylene surface. CSA-FFS – chitosan in aqueous acid solution; CSE-FFS – chitosan in hydroalcoholic acid solution; CSACVC-FFS – chitosan and carvacrol in aqueous acid solution; CSECVC-FFS – chitosan and carvacrol in hydroalcoholic acid solution.

The phenomenon of spreading of the liquid over the surface, as measured by the contact angle, is dependent on the relative magnitude of cohesive and adhesive molecular forces that exist respectively within the liquid and between the liquid and the solid: wetting is favoured by low γ_{LS} and γ_{LV}, and high γ_{SV} (Eq. (1)). Initially, after the deposition of different FFS, a significant modification of the liquid/PE film contact angle occurred. The same trend was monitored during all the recorded period (120 s) (Fig. 2). The

Table 2
Comparison of surface free energy and the dispersive (γ_S^D) and polar (γ_S^P) components of polyethylene film and chitosan self standing films. Measurement were done at air drying surface (air) and support drying surface (support).

Film sample	Surface free energy (mN/m)	γ_S^D (mN/m)	γ_S^P (mN/m)	Critical surface tension (mN/m)
PE	35.76	31.29	4.47	17.36
CSE air	37.32	36.12	1.20	41.80
CSE support	32.76	31.90	0.85	38.55
CSECVC air	66.42	43.72	22.70	76.68
CSECVC support	32.68	31.90	0.78	38.74
CSA air	39.69	38.59	1.10	44.35
CSA support	34.30	33.44	0.86	39.34
CSACVCair	65.29	36.00	29.30	76.54
CSACVC support	37.68	35.79	1.88	40.02

PE – polyethylene; CSA – chitosan film prepared with aqueous acid solution; CSE – chitosan film prepared with hydroalcoholic acid solution; CSACVC – chitosan film prepared from chitosan and carvacrol in aqueous acid solution; CSECVC – chitosan film prepared with chitosan and carvacrol in hydroalcoholic acid solution.

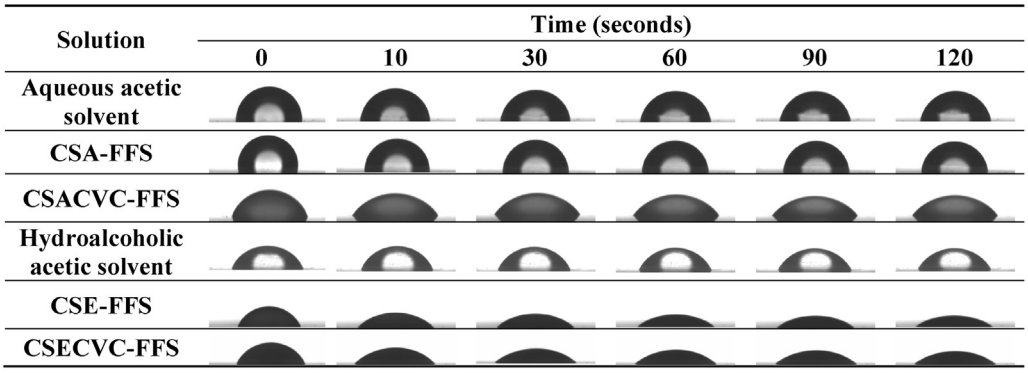

Fig. 2. Pictures of solvents and chitosan film forming solutions when applied to polyethylene film. CSA-FFS – chitosan in aqueous acid solution; CSE-FFS – chitosan in hydroalcoholic acid solution; CSACVC-FFS – chitosan and carvacrol in aqueous acid solution; CSECVC-FFS – chitosan and carvacrol in hydroalcoholic acid solution.

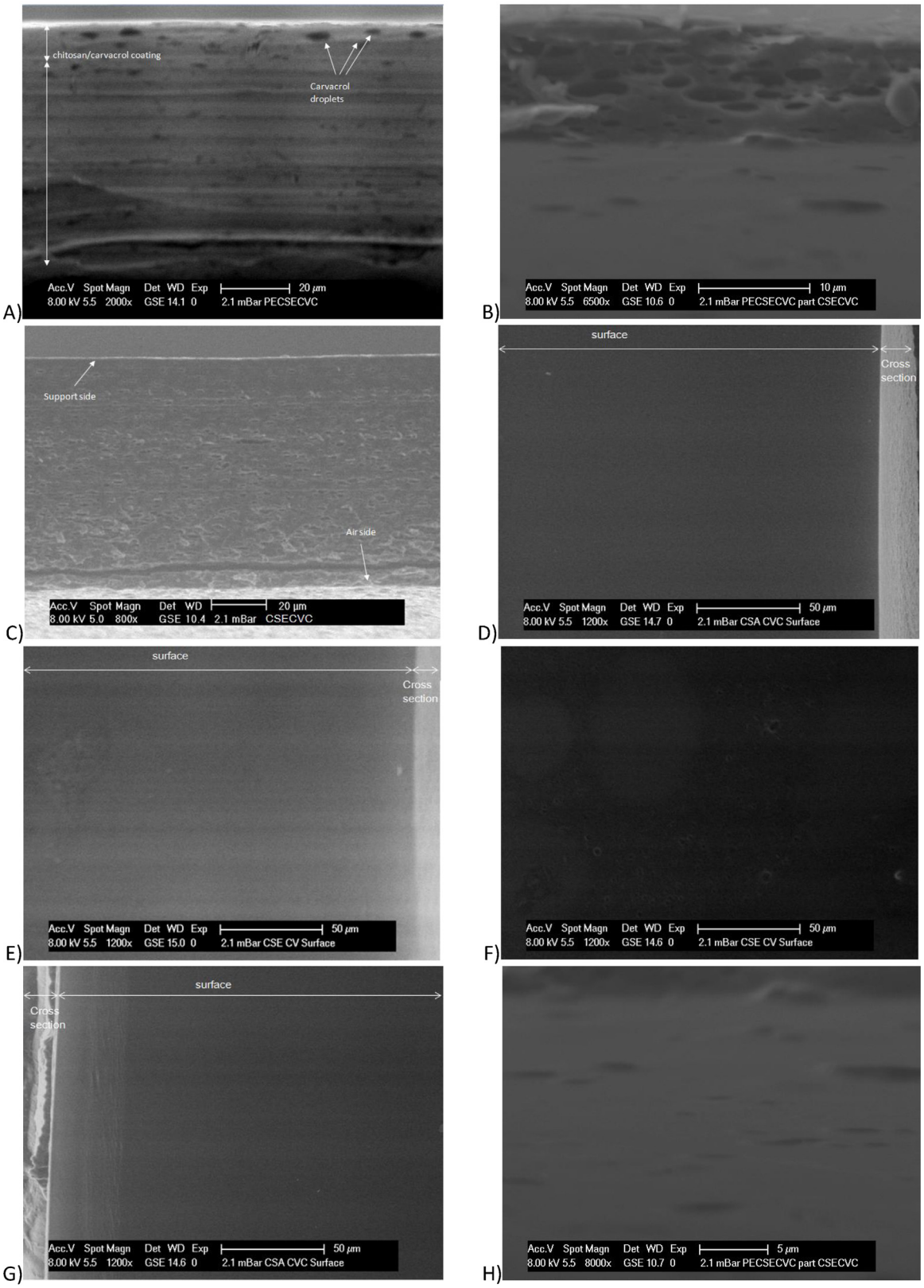

Fig. 3. ESEM cross sections of PECSECVC film (A), CSECVC coating layer (B), CSECVC film (C) and surfaces of chitosan films – support side surface of CSACVC (D) and CSECVC (E) and air side surface of CSECVC (F and H) and CSACVC (G). CSACVC – chitosan film prepared with aqueous acetic acid and carvacrol; CSECVC – chitosan film prepared with hydroalcoholic acid and carvacrol; PECSECVC – chitosan containing carvacrol coated PE film.

obtained contact angle values were lower than 90°, hence denoting a spontaneous partial wetting of the PE surface with all FFS (Hagenmaier & Baker, 1993). In addition, optimisation of wettability (W_s) includes optimisation of work of adhesion (W_a) and work of cohesion (W_c). Cohesion promotes contraction and adhesion promotes the spreading of a liquid. The obtained results are reported in Table 1. Higher cohesive force of a coating solution caused the shrinkage of the CSA droplet. In addition to the reduced superficial tension of the FFS (Table 1) the W_s was improved with the addition of ethanol and carvacrol (from −63.38 to −6.99). CSECVC had the highest W_s (the closest to zero), so it was considered as the most suitable solution to coat the PE surface (Tzoumaki, Biliaderis, & Vasilakakis, 2009). Since good stability between coating and PE occurred, the force required to separate the coating film from PE was increased. Thus the solution spread and good adhesion occurred (Fig. 3A). This phenomenon may be attributed to the adsorption of the surface active molecules in FFS at the liquid–vapour interface and its transfer to the solid–liquid interface during the coating process (Von Bahr, Tiberg, & Zhmud, 1999). Then spreading of CSECVC-FFS was increased and the contact angle decreased. Liquid surface tensions of hydroalcoholic coatings were closer to γ_C of the PE film. The lowest liquid surface tension value (31.3 mN/m) matched the lowest contact angle value (39°) and therefore, a better spreading and probably a better adhesion followed.

3.2. Surface free energy and critical surface tension of dry chitosan self standing films

To better understand the functional film properties, the hydrophilic/hydrophobic character of chitosan films (reported as the surface free energy) and the critical surface tension were determined. Results are given in Tables 1 and 2. The surface free energy controls the contact angle of the droplet with the film surface. Film air sides were more hydrophilic than film support sides (higher values of reported data) (Tables 1 and 2). Even though a hydrophobic behaviour should be expected in carvacrol containing films, CSECVC and CSACVC films had significantly higher surface free energies (66.4 and 65.3 mN/m, respectively). Other authors reported that the addition of hydrophobic agents, such as essential oils and lipids, could increase the surface hydrophobicity (Moradi et al., 2012; Ojagh, Rezaei, Razavi, & Hosseini, 2010). Opposite results in this study indicated that during drying process, some changes in the film structure occurred (Fig. 3) as well as new chemical interactions between components settled (Kurek, 2012). From Table 2, it can be seen that the polar component (γ_S^P) of air side chitosan surfaces changed up to 29 times after the incorporation of carvacrol (Table 2). This behaviour could be also due to the non-polar impurities on the chitosan surface (Farris et al., 2011). On top of that, the possible orientation of the methyl moieties of the residual acetyl groups along the chitosan backbone may have become exposed at the solid/air interface for the thermodynamic reasons (Cunha et al., 2008). Higher values of dispersive components, ranging from 31.90 mN/m for CSE support side to 43.72 mN/m for CSECVC air side are consistent with the typical values found for the polysaccharide films.

3.3. Film microstructure

Environmental scanning electronic microscopy observations were carried out to contribute to a better insight in the homogeneity and in the microscopic structure of dried films. The final microstructure is influenced by the structural arrangement of chitosan and carvacrol before and after drying. In the coated samples, a good adhesion was observed (Fig. 3A). According to Sánchez-González, González-Martínez, Chiralt, and Cháfer (2010), droplet flocculation, coalescence and creaming can occur. Layered structure of pure chitosan films was attributed to the orientation of chitosan chains in the matrix structure and to the evapouration front during drying (Kurek, Brachais, et al., 2012). Presence of carvacrol resulted in the heterogeneous structure (Fig. 3B). Carvacrol droplets were embedded in a continuous chitosan network. Besides, the heterogeneous structure could result in a lower stability of the FFS during drying. As the dry matter content increased, greater molecular contact between chitosan and carvacrol was obtained. Thus, formation of new interactions might weaken the polymer chain aggregation forces. The formed matrix was more opened so thicker films were formed (thickness increased up to 15% for CSECVC films). Fig. 3C shows that the upper part, corresponding to the evapouration surface during drying, exhibited a porous-like structure. This structure was also favoured by creaming of carvacrol droplet driven by solvent migration towards the evapouration surface. The lower part was more compact. The oval droplet form of carvacrol (Fig. 3A–C) was probably due to the deformation forces assigned to a polymer chain aggregation, network retraction and orientation during casting and the solvent evapouration. Surface micrographs indicated that the support side surfaces of all chitosan films were smooth and without cracks (Fig. 3D and E). Air side surface of CSACVC sample was smooth and homogeneous (Fig. 3G), while air side surface of CSECVC sample showed discontinuities (Fig. 3F). This indicated phase separation and orientation of carvacrol droplets to the evapourating surface. Surface convexity and presence of small holes, once again attributed to carvacrol were also observed (Fig. 3G and H).

3.4. Water vapour permeability

Polyethylene films are hydrophobic materials known to be not very permeable to water vapour. Therefore, it was interesting to verify the effect of the coating composition (carvacrol and chitosan) and of the processing onto the water vapour permeability of coated PE films. Previously, it was reported that hygroscopic chitosan layer that interacts easily with the surroundings, can act as a water reservoir on the PE surface. Thus it can significantly promote WVP of the support layer (Kurek, Ščetar, Voilley, Galić, & Debeaufort, 2012; Sebti, Chollet, Degrave, Noel, & Peyrol, 2007). The water vapour permeability values (measured at relative humidity gradient from 0 to 33% RH) for PE coated films are given in Fig. 4 and for self standing chitosan films in Table 3. No significant differences were observed when thin chitosan coating (6 μm) without carvacrol was applied on polyethylene film (7.72×10^{-13} and 7.88×10^{-13} g/m s Pa for PE and PECSE, respectively). Moreover, the WVP was increased by incorporating carvacrol into the coating layer. Indeed, the addition of a hydrophobic substance does not guarantee reduced WVP, because the permeability of the films is influenced by the existence of the free channelling for the diffusion of water molecules (Cheng, Abd Karim, & Seow, 2008; Pereda, Amica, & Marcovich, 2012). The WVP trend of self standing chitosan films was similar to the coated samples. In carvacrol containing samples, the WVP increased for about five times. It is possible that carvacrol induced a plasticisation of the chitosan network, decreased intermolecular attractions and increased molecular mobility (denoted by the thermal analysis in parallel study). Then the migration of water vapour molecules was facilitated. Furthermore, it is generally recognised that the WVP of biopolymer films strongly depends on their thickness (McHugh, Avena-Bustillos, & Krochta, 1993). Accordingly, WVP of thicker films was also higher (Table 3). Another possible explanation for this behaviour could be the formation of porous structure with the addition of carvacrol as revealed by ESEM data (Fig. 3). In the literature, different effects of aroma compounds on WVP were reported. According to Bonilla, Atarés, Vargas, and Chiralt (2012) and Martins, Cerqueira, and Vicente (2012), the incorporation of

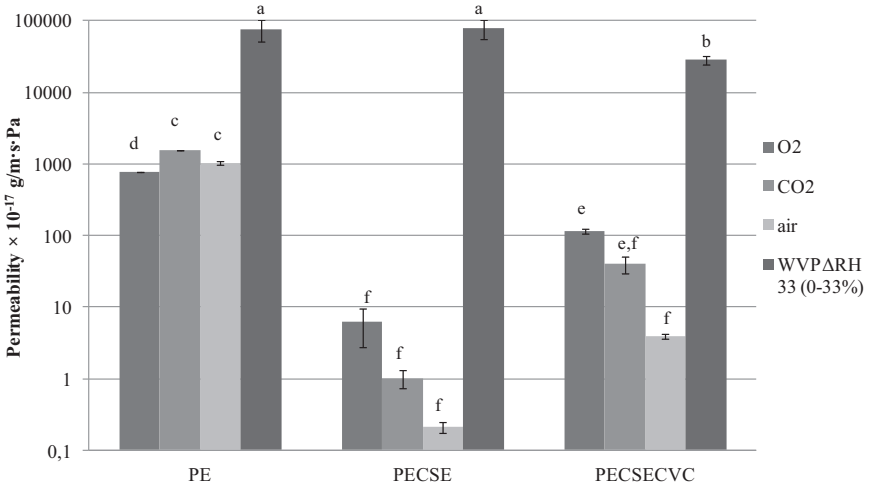

Fig. 4. Water vapour (WVP), oxygen, carbon dioxide and air permeability of polyethylene (PE), chitosan coated (PECSE) and chitosan + carvacrol coated (PECSECVC) polyethylene film. Different superscript letters indicate significant differences between formulations ($p < 0.05$).

essential oils had the negative effect on cohesion forces of the chitosan matrix. This explains the phenomena of enhanced transport through the film despite the increase of the hydrophobic character of the matrix. WVP of soy protein or alginate based films was increased by the presence essential oils while the addition of aroma compounds decreased WVP of carrageenan based films (Atarés, De Jesús, Talens, & Chiralt 2010; Hambleton, Debeaufort, Beney, Karbowiak, & Voilley, 2008; Rojas-Grau et al., 2007). In this study, the difference between hydroalcoholic and aqueous acidic samples (CSE and CSA) was also observed. Ethanol in FFS could modify the film structure because of the variation in the polarity and the interfacial tension. Ethanol also influenced the solubility of chitosan powder, so WVP of dry films was increased.

3.5. Oxygen, carbon dioxide and air permeability

One of the most interesting applications of chitosan based films is their high gas barrier properties. It governs gas transfers between food products and their surroundings. Gas permeability properties could be changed by the addition of active compounds that can act as structure enhancers. Oxygen, carbon dioxide and air permeability of chitosan coated PE at 25 °C in the dry conditions (to prevent moisture plasticisation of the chitosan) are given in Fig. 4. Permeability data for self standing chitosan films are given in Table 3. P_{CO_2} of PE film was two times higher than P_{O_2} (Fig. 4). Chitosan coating on PE surface decreased oxygen, carbon dioxide and air permeability from two to four orders of magnitude, respectively. This decrease was undoubtedly attributed to the presence of the thin chitosan layer (6 μm). The presence of carvacrol in the chitosan layer increased ten times the P_{O_2}, P_{CO_2} and P_{air}. In theory, gas permeability of biopolymer films depends on factors such as film integrity, crystalline/amorphous phase ratio, hydrophilic/hydrophobic ratio, chain mobility and interaction between polymer and added molecules. These factors in combination can change the matrix structure (Garcıa, Martino, & Zaritzky, 2000). In the present study, two possible explanations are given. According to Gennadios (2002) permeability is a steady state property that describes the extent to which a permeating substance dissolves and then the rate at which it diffuses through a film. Firstly, the increase in the permeability with the addition of carvacrol was associated to the breakdown of hydrogen bonds between the chitosan polymer chains. Then additional sites for the dissolution of gases were opened and the mobility of oxygen molecules within the chitosan layer was increased. As a second point, the increase could be explained by gas solubility in the nonpolar carvacrol domains. Similarly, Farris, Introzzi, and Piergiovanni (2009) noticed that the addition of the hydrophobic oil molecules decreased the density of protein network. Therefore, less tight lattices were formed and small gas molecules passed faster across the sample. However, all coated samples were significantly less permeable than uncoated PE. Their permeabilities were in the same order: $P_{O_2} > P_{CO_2} > P_{air}$. In addition, P_{O_2} was decreased with the temperature decrease. As temperature increased, molecules had more energy, so they could easily pass through both the PE film and the chitosan coating. Also it is possible that thermal expansion of the polymer material occurred (Rogers, 1985). Oxygen permeation through the chitosan coated PE films without carvacrol was more sensitive to temperature changes than that of commercial PE and chitosan coated PE with incorporated carvacrol (14 and 2 times higher at 25 °C, respectively, data not shown). Hence, activation energies (E_a) decreased in the following order: $E_{aPECSE} > E_{aPE} > E_{aPECSECVC}$ (87.8, 28.4 and 27.2 kJ/mol respectively).

Theoretically, from the permeability data for individual components it is possible to calculate the permeability of the coating

Table 3
Film thickness, water vapour (WVP), oxygen (P_{O_2}), carbon dioxide (P_{CO_2}) and air permeability (P_{air}) of chitosan self standing films.

Sample	Film thickness (μm)	WVP ($\times 10^{-13}$ g/m s Pa) ΔRH (0–33%)	P_{O_2} ($\times 10^{-17}$ g/m s Pa)	P_{CO_2} ($\times 10^{-17}$ g/m s Pa)	P_{air} ($\times 10^{-17}$ g/m s Pa)
CSE	65 ± 4	38.71 ± 2.61b	2.22 ± 0.27b	1.49 ± 0.17c	0.22 ± 0.05d
CSECVC	80 ± 6	189.91 ± 74.65a	2.72 ± 0.33b	3.77 ± 0.09b	4.35 ± 0.19b
CSA	55 ± 2	25.71 ± 2.20b	1.04 ± 0.15c	6.98 ± 0.81a	3.79 ± 0.25c
CSACVC	81 ± 5	101.48 ± 40.59a,b	8.19 ± 0.51a	7.76 ± 0.39a	5.69 ± 0.24a
CSE (calculated)	6	/	0.73	0.12	0.63
CSECVC (calculated)	6	/	17	5.18	0.49

Different letters within the columns indicate significant differences between formulations ($p < 0.05$).
CSA – chitosan film prepared with aqueous acid solvent; CSE – chitosan film prepared with hydroalcoholic acid solvent; CSACVC and CSECVC – carvacrol containing films.

layer from film thickness. Calculated values are given in Table 3. Comparison with the experimental data was difficult since with the applied procedure, it was impossible to produce self standing films with the same thickness as the coating layer. Even though theoretically gas permeabilities of a particular type of film are independent of the film thickness (Schwartzberg, 1986), in a practice, various reasons for thickness effects in biopolymer films have been reported. Different preparation of self standing and coated films and possible structure changes with the film thickness might influence film performance. Thus, the deviation between experimental and calculated data occurred.

Taking into account only self standing films, it was observed that when films were produced from hydroalcoholic solvent P_{CO_2} and P_{air} were lower. This was attributed to the structural orientation, conformation changes in the chitosan matrix and probably to the densification of the chitosan network and confirmed by FTIR and DSC (unpublished data, Kurek, 2012). The film structure as well as the distribution of carvacrol oil droplets might be associated with the gas and water vapour permeability of the resulting films (Fig. 3). The permeability of carvacrol containing self standing films was significantly higher than CSE and CSA films (Table 3). Nevertheless when compared with synthetic materials, the permeabilities of all chitosan self supported films remained weak and could be used as good barrier coating materials.

4. Conclusions

For production of novel bilayer/PE films with improved characteristics and then active properties, the knowledge of wetting properties represents a key parameter to enhance their aptitude to adhere to plastic layer, while maintaining the integrity of packaging. Chitosan biopolymer film forming solutions spread and partially wet the polyethylene film surface. During the period of 120 s measurements revealed contact angles lower than 90°. Indeed, these characteristics are primarily influenced by surface wettability of films which is dependent upon the degree of contact achieved between plastic surfaces and wetting film forming solution. Furthermore, the magnitude of intermolecular forced involved plays important role. Then, hydroalcoholic acid solvent and carvacrol decreased the liquid surface tension of CSE and CSECVC film forming solutions, increased the solution surface pressure and spreading and decreased the contact angle. Then, the equilibrium-spreading coefficient was improved. Therefore, the chitosan film forming solution containing ethanol and carvacrol as surface active components was considered as the most suitable for polyethylene coating. Environmental scanning microscopy indicated that carvacrol containing films had heterogeneous structure with two phases. Carvacrol droplets were embedded in the chitosan matrix. The presence of carvacrol might have decreased intermolecular attractions and increased molecular mobility. Furthermore, the film structure as well as the distribution of carvacrol droplets was associated with facilitated migration of water vapour and gas molecules. Ethanol affected the chitosan powder solubility and the water vapour permeability of dry films was increased. Chitosan layer, as carbohydrate based polymer, significantly decreased the gas permeabilities of the polyethylene film. Carvacrol increased P_{O_2}, P_{CO_2} and P_{air} of PE coated samples for ten times, following the order $P_{O_2} > P_{CO_2} > P_{air}$.

Acknowledgments

The authors wish to thank the colleagues from PAM-PAPC Laboratoire. The authors special thanks to Dr Alain Guinault for pilot coating process and Mme Aline Bonnotte for ESEM. This work was supported by the Ministère de l'Enseignement Supérieur et de la Recherche, the Ministère de l'Economie, de l'Industrie et de l'Emploi, by the way of Fond Unique Interministériel (project EMAC No. 09 290 6395), the Conseil Régional de Bourgogne, Direction Générale de la Competitivite de l'Industrie et des Services, Conseil régional Franche-Comté, Conseil Régional Picardie, Conseil Général Côte d'Or, Conseil Général du Jura, le Grand Dijon, the competitive clusters Vitagora, IAR et Plastipolis and all private partners involved in this project. The authors wish to thank Prof. JP Gay for English improvement.

References

Arvanitoyannis, I. S. (1999). Totally and partially biodegradable polymer blends based on natural and synthetic macromolecules: Preparation, physical properties, and potential as food packaging materials. *Journal of Macromolecular Science – Reviews in Macromolecular Chemistry and Physics, C 39*(2), 205–271.

Atarés, L., De Jesús, C., Talens, P., & Chiralt, A. (2010). Characterization of SPI-based edible films incorporated with cinnamon or ginger essential oils. *Journal of Food Engineering, 99*, 384–391.

Bonilla, J., Atarés, L., Vargas, M., & Chiralt, A. (2012). Effect of essential oils and homogenization conditions on properties of chitosan-based films. *Food Hydrocolloids, 26*, 9–16.

Cheng, L. H., Abd Karim, A., & Seow, C. C. (2008). Characterisation of composite films made of konjac glucomannan (KGM), carboxymethyl cellulose (CMC) and lipid. *Food Chemistry, 107*, 411–418.

Cunha, A. G., Fernandes, S. C. M., Freire, C. S. R., Silvestre, A. J. D., Neto, C. P., & Gandini, A. (2008). What is the real value of chitosan's surface energy? *Biomacromolecules, 9*, 610–614.

Debeaufort, F., Martin-Polo, M. O., & Voilley, A. (1993). Polarity homogenicity and structure affect water vapour permeability of model edible films. *Journal of Food Science, 58*, 426–434.

Dupre, A. (1869). *Theorie Mecanique de La Chaleur*. Paris: Gauthier-Villan.

Farris, S., Introzzi, L., & Piergiovanni, L. (2009). Evaluation of a biocoating as a solution to improve barrier, friction and optical properties of plastic films. *Packaging Technology and Science, 22*, 69–83.

Farris, S., Introzzi, L., Biagioni, P., Holz, T., Schiraldi, A., & Piergiovanni, L. (2011). Wetting of biopolymer coatings: Contact angle kinetics and image analysis investigation. *Langmuir, 27*, 7563–7574.

Garcıa, M. A., Martino, M. N., & Zaritzky, N. E. (2000). Microstructural characterization of plasticized starch-based films. *Starch–Stärke, 52*, 118–124.

Gennadios, A. (2002). *Protein-based films & coatings*. CRC Press.

Hagenmaier, R. D., & Baker, R. A. (1993). Reduction in gas exchange of citrus fruit by wax coatings. *Journal of Agriculture and Food Chemistry, 41*, 283–287.

Hambleton, A., Debeaufort, F., Beney, L., Karbowiak, T., & Voilley, A. (2008). Protection of active aroma compound against moisture and oxygen by encapsulation in biopolymeric emulsion-based edible films. *Biomacromolecules, 9*(3), 1058–1063.

Hong, S. I., & Krochta, J. M. (2006). Oxygen barrier performance of whey-protein coated plastic films as affected by temperature, relative humidity, base film and protein type. *Journal of Food Engineering, 77*, 739–745.

Hong, S. I., Lee, J. W., & Krochta, J. M. (2005). Properties of polysaccharide-coated polypropylene films as affected by biopolymer and plasticizer type. *Packaging Technology and Science, 18*, 1–9.

Kaelble, D. H. (1970). Dispersion-polar surface tension properties of organic solids. *Journal of Adhesion, 2*, 66–81.

Karbowiak, T., Debeaufort, F., & Voilley, A. (2006). Importance of surface tension characterization for food, pharmaceutical and packaging products: A review. *Critical Reviews in Food Science and Nutrition, 46*, 1–17.

Kurek, M. v. (2012). *Comprehensive study of the effects of formulation and processing parameters on structural and functional properties of active bio-based packaging films*. University of Burgundy and University of Zagreb. PhD Thesis.

Kurek, M., Brachais, C.-H., Nguimjeu, C. M., Bonnotte, A., Voilley, A., Galić, K., et al. (2012). Structure and thermal properties of a chitosan coated polyethylene bilayer film. *Polymer Degradation and Stability, 97*(8), 1232–1240.

Kurek, M., Ščetar, M., Voilley, A., Galić, K., & Debeaufort, F. (2012). Barrier properties of chitosan coated polyethylene. *Journal of Membrane Science, 403*, 162–168.

Martins, J. T., Cerqueira, M. A., & Vicente, A. A. (2012). Influence of a-tocopherol on physicochemical properties of chitosan-based films. *Food Hydrocolloids, 27*, 220–227.

McHugh, T. H., Avena-Bustillos, R. J., & Krochta, J. M. (1993). Hydrophilic edible film: Modified procedure for water vapor permeability and explanation of thickness effects. *Journal Food Science, 58*, 899–903.

Moradi, M., Tajik, H., Razavi Rohani, S. M., Rasoul Oromiehie, A., Malekinejad, H., & Aliakbarlu Hadian, J. M. (2012). Characterization of antioxidant chitosan film incorporated with Zataria multiflora Boiss essential oil and grape seed extract. *LWT – Food Science and Technology, 46*, 477–484.

Ojagh, S. M., Rezaei, M., Razavi, S. H., & Hosseini, S. M. H. (2010). Development and of a novel biodegradable film made from chitosan and cinnamon essential oil with low affinity toward water. *Food Chemistry, 122*, 161–166.

Owens, D. K., & Wendt, R. C. (1969). Estimation of the surface free energy of polymers. *Journal of Applied Polymer Science, 13*, 1741–1747.

Pereda, M., Amica, G., & Marcovich, N. E. (2012). Development and characterization of edible chitosan/olive oil emulsion films. *Carbohydrate Polymers*, *87*, 1318–1325.

Rabel, W. (1971). Einige aspekte der benetzungstheorie und ihre anwendung auf die untersuchung und veranderung der oberflacheneigenschften von polymeren. *Farbe und Lack*, *77*(10), 997–1006.

Rogers, C. E. (1985). Permeation of gases and vapours in polymers. In J. Comyn (Ed.), *Polymer permeability* (pp. 11–73). New York: Elsevier Applied Science Publishers.

Rojas-Grau, M., Raybaudi-Massilia, R. M., Soliva-Fortuny, R. S., Avena-Bustillos, R. J., McHugh, T. H., & Martın-Belloso, O. (2007). Apple puree-alginate edible coating as carrier of antimicrobial agents to prolong shelf-life of fresh-cut apples. *Postharvest Biology and Technology*, *45*, 254–264.

Rulon, J., & Robert, H. (1993). Wetting of low-energy surfaces. In J. C. Berg (Ed.), *Wettability* (pp. 4–73). Seattle: Marcel Dekker Inc.

Sánchez-González, L., González-Martínez, C., Chiralt, A., & Cháfer, M. (2010). Physical and antimicrobial properties of chitosan-tea tree essential oil composite films. *Journal of Food Engineering*, *98*, 443–452.

Schwartzberg, H. G. (1986). Modeling of gas vapour transport through hydrophilic films. In M. Mathlouthi (Ed.), *Food Packaging and Preservation. Theory and Practice*. London: Elsevier Applied Science.

Sebti, I., Chollet, E., Degrave, P., Noel, C., & Peyrol, E. (2007). Water sensitivity, antimicrobial, and physicochemical analyses of edible films based on HPMC and/or chitosan. *Journal of Agricultural and Food Chemistry*, *55*, 693–699.

Siripatrawan, U., & Harte, B. R. (2010). Physical properties and antioxidant activity of an active film from chitosan incorporated with green tea extract. *Food Hydrocolloids*, *24*.

Sollogoub, C., Guinault, A., Bonnebat, C., Bennjima, M., Akrour, L., Fauvarque, J. F., et al. (2009). Formation and characterization of crosslinked membranes for alkaline fuel cells. *Journal of Membrane Science*, *335*, 37–42.

Song, B., & Springer, J. (1996a). Determination of interfacial tension from the profile of a pendant drop using computer-aided image processing 1. Theoretical. *Journal of Colloid and Interface Science*, *184*(1), 64–76.

Song, B., & Springer, J. (1996b). Determination of interfacial tension from the profile of a pendant drop using computer-aided image processing 1. Experimental. *Journal of Colloid and Interface Science*, *184*(1), 77–91.

Suyatma, N. E., Copinet, A., Tighzert, L., & Coma, V. (2004). Mechanical and barrier properties of biodegradable films made from chitosan and poly(lactic acid) blends. *Journal of Polymers and the Environment*, *12*(1), 1–6.

Suppakul, P., Miltz, J., Sonneveld, K., & Bigger, S. (2003). Active packaging technologies with an emphasis on antimicrobial packaging and its applications. *Journal of Food Science*, *68*, 408–420.

Tharanathan, R., & Kittur, F. (2003). Chitin – the undisputed biomolecule of great potential. *Critical Reviews in Food Science*, *43*(1), 61–87.

Tzoumaki, M. V., Biliaderis, C. G., & Vasilakakis, M. (2009). Impact of edible coatings and packaging on quality of white asparagus (*Asparagus officinalis*, L.) during cold storage. *Food Chemistry*, *117*, 55–63.

Van Oss, C. J. (1994). *Interfacial forces in aqueous media*. New York: Marcel Dekker.

Vargas, M., Albors, A., Chiralt, A., & González-Martínez, C. (2009). Characterization of chitosan–oleic acid composite films. *Food Hydrocolloids*, *23*, 536–547.

Von Bahr, M., Tiberg, F., & Zhmud, B. V. (1999). Spreading dynamics of surfactant solutions. *Langmuir*, *15*, 7069–7075.

Young, T. (1805). An essay on the cohesion of fluids. *Philosophical Transactions of the Royal Society*, *95*, 65–87.

Zenkiewicz, M. (2007). Methods for the calculation of surface free energy of solids. *Journal of Achievements in Materials and Manufacturing Engineering*, *24*(1), 137–145.

Ziani, K., Oses, J., Coma, V., & Maté, J. I. (2008). Effect of the presence of glycerol and Tween 20 on the chemical and physical properties of films based on chitosan with different degree of deacetylation. *LWT – Food Science and Technology*, *41*, 2159–2165.

Zisman, W. A. (1964). Contact angle wettability and adhesion. In R. F. Gould (Ed.), *Advances in chemistry series* (pp. 1–5). Washington, DC: American Chemical Society.